






Cite this: *Chem. Commun.*, 2021, 57, 5662

Received 17th March 2021,
Accepted 29th April 2021

DOI: 10.1039/d1cc01452h

rsc.li/chemcomm

Quantitative helix handedness bias through a single H vs. CH₃ stereochemical differentiation†

Daniel Bindl,  Elisabeth Heinemann, Pradeep K. Mandal  and Ivan Huc *

A novel chiral aromatic δ -amino acid building block was shown to fully induce handedness in quinoline oligoamide foldamers with the possibility of further increasing the bias by combining multiples of these units in the same sequence. Through its incorporation within the helix, both N- and C-termini are still accessible for further functionalisation.

Handedness control in aromatic foldamer helices is of prime importance for their applications in circularly polarized luminescence,^{1,2} enantioselective catalysis,³ and the diastereoselective recognition of chiral guests either within an internal cavity^{4,5} or at their surfaces as, for example, proteins.^{6–10} Promoting minimal handedness bias is straightforward: most stereogenic centers placed in the vicinity of the helix backbone will create an energy imbalance in favor of one or the other helix sense.¹¹ Only 1 kJ mol^{−1} is required to elicit a 60/40 ratio. In contrast, quantitative handedness control, *i.e.* a diastereomeric excess of at least 99%, has rarely been achieved because it requires a large energy difference between *P*- and *M*-helical diastereomers. The few examples reported concern aromatic oligoamide foldamers derived from 8-amino-2-quinolinecarboxylic acid (**Q_n**) (Fig. 1a) possessing N- or C-terminal chiral moieties such as camphanyl (Camph),¹² oxazolyaniline (Oxaz)^{3,13} or β -pinene-derived pyridyl (Pin)¹⁴ groups (Fig. 1b). All these moieties incorporate stereogenic centers embedded within a cyclic system and form hydrogen bonds with a main chain amide. Terminal functionalization by a chiral moiety is often convenient, but it can hamper other functionalizations, *e.g.* with a chromophore, a protein ligand, in particular in the context of protein surface recognition.^{7–10} Here we show that 2-(2-aminophenoxy)-propionic acid monomer **B^{Rme}** (Fig. 2a) promotes quantitative handedness induction in water when embedded *within* an aromatic oligoamide helix sequence.

Department of Pharmacy and Center for Integrated Protein Science,
Ludwig-Maximilians-Universität, Butenandtstraße 5-13, München 81377, Germany.
E-mail: ivan.huc@cup.lmu.de

† Electronic supplementary information (ESI) available: Synthetic and crystallographic procedures. CCDC 2070816. For ESI and crystallographic data in CIF or other electronic format see DOI: 10.1039/d1cc01452h

Handedness bias is thus achieved through the stereochemical differentiation of a single main chain hydrogen atom and a methyl group. This strong effect illustrates that the compactness of aromatic helices allows for stronger stereochemical differentiation than in peptidic helices in which a single alanine residue is unable to achieve complete handedness bias of an otherwise achiral sequence.¹⁵

We speculated that placing a stereogenic center within an aromatic helix may result in strong helix handedness bias due to stereochemical constraints both above and below the chiral group. Nevertheless, a few earlier attempts failed to reach quantitative handedness control, perhaps due to the fact that the chiral groups were not themselves sufficiently helicogenic; that is, their presence may cause a partial helicity disruption.^{16–19} Chiral monomer **B^{Rme}** was designed as a δ -peptidic analogue of **Q** bearing a stereogenic center at a position expected to be at the inner rim of the helix. Its achiral equivalent, 2-(2-aminophenoxy)-acetic acid, has already been described,²⁰ and homomeric sequences of this monomer have been shown to fold not into a

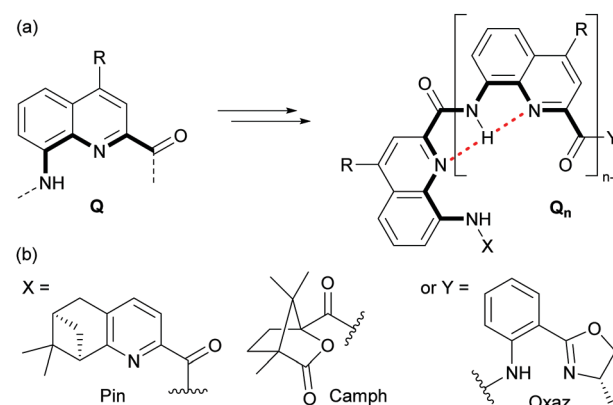


Fig. 1 (a) Chemical structures of **Q** and its oligomer **Q_n**. Backbone hydrogen bonds are indicated by red dashed lines. (b) N-terminal groups (X) and C-terminal groups (Y), which are known to fully induce one handedness in **Q_n** oligomers.^{12–14}

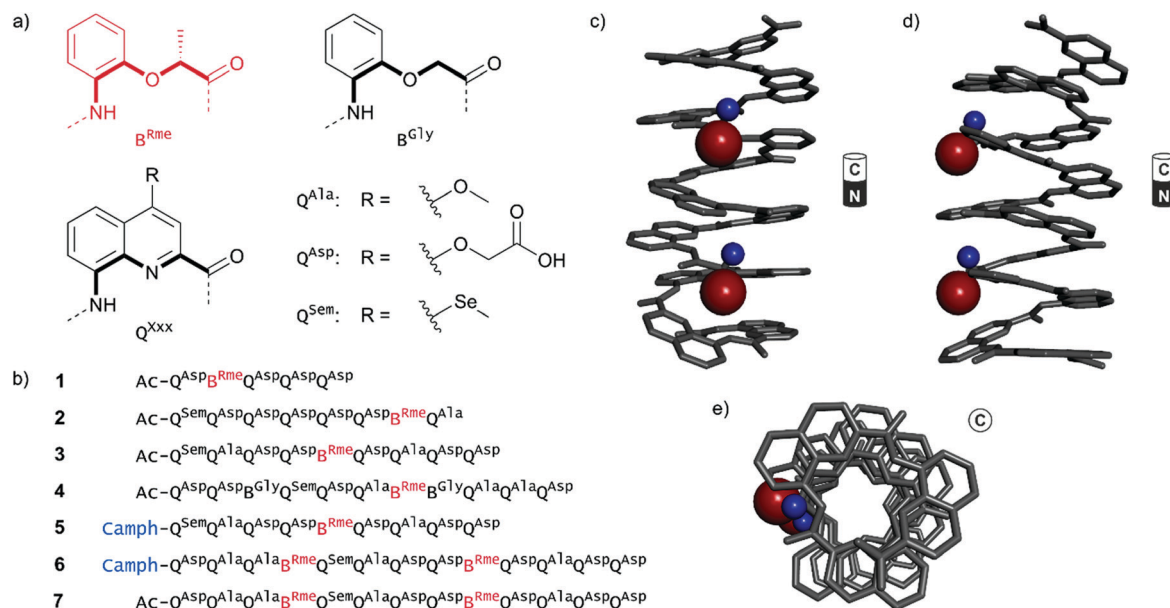


Fig. 2 (a) Foldamer building blocks used in this study. (b) Sequences that were synthesized to investigate the handedness induction properties of B^{Rme} . The chiral units (S)-Camph and B^{Rme} are shown in blue and red, respectively. (c–e) Crystal structure of oligomer **7** in side (c and d) and top (e) views showing a canonical aromatic helix structure. Side chains and hydrogen atoms are omitted for clarity. The methyl group (red) and hydrogen atom (blue) on the chiral center of B^{Rme} are represented as balls. The N- and C-terminus orientations are shown next to the respective structure.

canonical aromatic helix, but into a herringbone-helical structure.^{20,21} However, it is also known that Q_n sequences can template the canonical helical folding of other monomers.^{19,22,23} We thus endeavored to prepare an Fmoc protected version of B^{Rme} and to incorporate it into Q_n oligomers to investigate its ability to bias helix handedness.

Two new monomers, Fmoc- B^{Rme} -OH and Fmoc- B^{Gly} -OH, were synthesized from *ortho*-nitrophenol in 91% and 36% overall yield in four steps, respectively (Fig. S1, ESI†). The stereogenic center of B^{Rme} was installed by condensing ethyl (–)-L-lactate to 2-nitrophenol *via* a Mitsunobu reaction leading to an inversion of the stereochemistry. A derivatization of the final Fmoc- B^{Rme} -OH with a chiral amine confirmed that the enantiomeric purity of the starting alcohol as given by the supplier ($\geq 97.5\%$) was preserved throughout the whole synthesis (Section S2, ESI†). An unanticipated difficulty had to be overcome during the preparation of Fmoc- B^{Rme} -OH and Fmoc- B^{Gly} -OH. The Mitsunobu product is a nitro ester that must undergo nitro group reduction and ester saponification prior to Fmoc installation. When performing reduction first, we found that the amino-ester readily cyclizes into a six-membered lactam. Even when saponification was carried out first, the amino-acid was quantitatively converted into the same lactam during nitro group hydrogenation (Fig. S1, ESI†). This unusual reactivity might explain the scarce record of **B** oligomers in the literature. Two different approaches were applied to circumvent this side reaction. First, for B^{Gly} , the cyclisation was partially prevented by using a bulky *tert*-butyl ester in the reduction step. For B^{Rme} , saponification was carried out first and a base (Na_2CO_3) was added during the hydrogenation to produce the sodium carboxylate salt. This entirely prevented lactam formation. These synthetic routes should be extendable to a

variety of **B** analogs bearing different chiral functionalities and/or side chains on the aromatic ring.

Sequences 1–7 were designed and synthesized to study the effect of one or two B^{Rme} units placed at various positions in sequences of variable lengths (Fig. 2b). Acidic Q^{Asp} monomers were introduced to provide solubility in aqueous media. To prevent too high solubility that could hamper crystal growth, some Q^{Ala} units were also included in the sequences so as to be positioned on different faces of the helix. In some sequences, one Q^{Sem} moiety containing a selenium atom was included to eventually enable the use of anomalous X-ray scattering, though this proved to be unneeded. Synthesis was performed on low loading Wang resin (100–200 mesh) using previously reported solid phase foldamer synthesis (SPFS) protocols.^{24,25} Fmoc acid building blocks were activated *in situ* by generating the respective acid chlorides prior to coupling. Both Fmoc- B^{Rme} -OH and Fmoc- B^{Gly} -OH showed excellent coupling reactivity. No noteworthy deletions occurred during SPFS. In a final step, the oligomers were cleaved from the resin and deprotected under acidic conditions. The crude oligomers were purified using semi-preparative reverse phase HPLC with a basic ammonium acetate buffer as the mobile phase. As a result, all compounds were obtained as their respective ammonium salts in good overall purified yields (8.4–51%; Section S3.2, ESI†).

As outlined in the introduction, we expected that the strong helicogenic nature of quinoline units would force the B^{Rme} and B^{Gly} monomers into canonical helical folding despite their steric demand and increased flexibility that results in a herringbone helix for $(B^{Gly})_n$.²⁰ NMR and circular dichroism (CD) spectroscopic data suggest that 1–7 all adopt a helical fold in water. They show the characteristic pattern of distinct amide

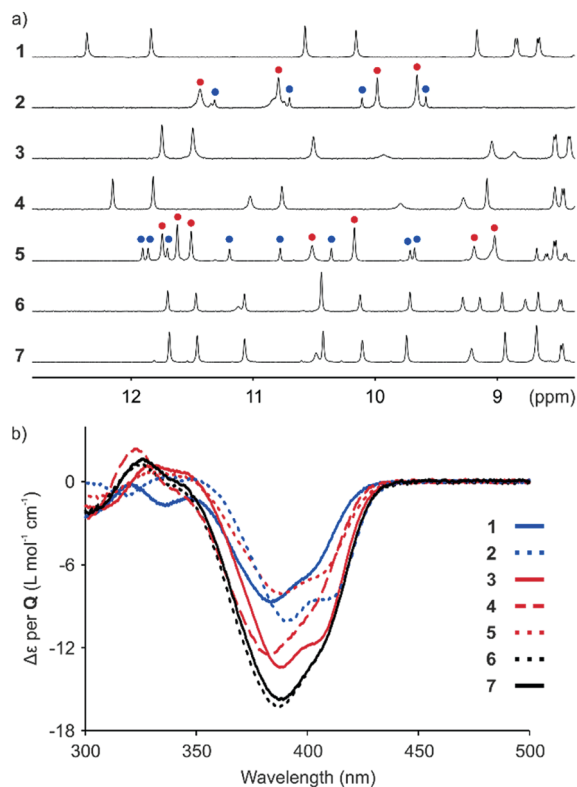


Fig. 3 (a) Amide region of the ^1H NMR spectra of sequences **1–7** in NH_4OAc buffer pH 8.5. For **2** and **5**, major and minor sets of signals are marked with red and blue circles, respectively. (b) CD spectra of compounds **1–7** in NH_4OAc buffer pH 8.5 between 300 and 500 nm. The molar extinction ($\Delta\epsilon$) is normalized for the number of **Q** units for better comparability.

and aromatic signals in their ^1H NMR spectra and an intense CD band in the 300–450 nm region that is typical for helically folded quinoline oligomers with some handedness bias^{12,26} (Fig. 3 and Fig. S2, ESI[†]). These findings are corroborated by the strongly downfield shifted ^1H NMR signals (between -0.18 and -0.33 ppm) of the CH_3 protons of B^{Rme} units in the spectra of **3–7** (Fig. S2, ESI[†]), as a result of the ring current effects of neighbouring **Q** units. For comparison, the signal of the same methyl group in $\text{Fmoc-B}^{\text{Rme}}\text{-OH}$ is found at 1.56 ppm. Similar upfield shifts are observed for protons close to aromatic side chains in proteins.²⁷

The helix conformation was also validated by the solid state structure of **7**, an analogue of **6** bearing an acetyl group instead of (*S*)-Camph (Fig. 2c–e). The structure shows canonical helical folding, with only left-handed helices present in the crystal. This structure was solved despite the low resolution of the data (2.86 \AA) by molecular replacement using an energy minimized model (Section S4, ESI[†]). Molecular replacement is a common phasing method in protein crystallography where models are produced from related structures, but it has scarcely been used for smaller molecules.²⁸ Successful molecular replacement in the case of **7** is a highlight of the effectiveness of molecular modelling at accurately predicting aromatic foldamer conformations, and represents an important methodological advance.

Helix handedness bias in solution was first assessed when B^{Rme} was placed in the penultimate position to the N- or

C-terminus of a sequence, as in **1** and **2**. Since one helix turn contains 2.5 units, the penultimate residue is entirely exposed to the solvent on one of its faces. The ^1H NMR spectrum of **1** shows one major set of signals (Fig. 3a), indicating a diastereomeric ratio of (*R*)-*M* to (*R*)-*P* of at least 98/2, assuming that the helix handedness inversion is slow on the NMR timescale, as expected for a pentamer or any longer sequence.⁹ The negative band observed by CD in the 300–450 nm region shows that the *M* helicity is dominant.²⁶ In the *M* helix, the asymmetric methyl group of **1** should ‘stick out’ of the helix towards the solvent. For **2**, the ^1H NMR spectrum shows two sets of signals with a ratio of about 87/13 (Fig. 3a). The CD spectrum indicates that the *M* helix is again dominant (Fig. 3b), which means that the asymmetric methyl this time points towards the helix and not to the solvent, since B^{Rme} is near the C terminus. The handedness preference thus depends on the absolute stereochemistry of B^{Rme} regardless of its position in the sequence, and not on whether the methyl groups point towards the helix or the solvent. We also note that the CD intensity does not correlate well with the diastereomeric excess. The CD band at 380 nm normalized per **Q** unit is more intense for **2** than for **1** although the handedness bias is stronger for the latter (Fig. 3b). Indeed, the CD intensity also depends on the number of consecutive **Q** units and on the nature of substituents on each **Q** unit.

Compounds **3** and **4** contain one B^{Rme} unit flanked with helix segments that span more than one turn. The asymmetric center should thus have close contacts with aryl groups both above and below. Sequence **4** was designed to be more flexible than **3**, due to additional achiral B^{Gly} units, including one adjacent B^{Rme} . The higher flexibility arises from the reduced aromatic stacking surface and additional rotatable bonds in **B** monomers as compared to **Q**. The ^1H NMR spectra of **3** and **4** both show a single set of sharp signals (Fig. 3a). This indicates quantitative handedness bias as far as NMR can detect. CD shows that **3** and **4** are *M* helical (Fig. 3b), as for **1** and **2**. Quantitative handedness bias achieved by the stereochemical differentiation between a hydrogen atom and a simple methyl group is remarkable and unprecedented. It probably results from the very compact conformation of Q_n helices that create a large energy difference between the diastereomeric conformers. Furthermore, NMR and CD concur to show that the handedness bias for compound **3** is also quantitative in DMSO and MeOH (Fig. S4, ESI[†]).

Encouraged by these results, we challenged handedness bias due to B^{Rme} through the introduction of an N-terminal camphanyl group having an (*S*) configuration, that is, a configuration antagonistic to that of B^{Rme} . In the absence of B^{Rme} , the camphanyl group also biases handedness quantitatively and its (*S*) configuration favors *P* helicity.¹² Sequence **5** is an analog of **3** where the terminal Ac has been replaced with (*S*)-Camph. Its ^1H NMR spectrum shows two sets of signals with a ratio of 75/25 corresponding to the presence of two different diastereomeric conformations, (*S,R*)-*M* and (*S,R*)-*P* (Fig. 3a). The CD spectrum shows a negative band in the range of 300–450 nm; this indicated that the major conformation has *M* handedness, and thus that B^{Rme} imparts a stronger handedness induction

than (*S*)-Camph (Fig. 3b). Because **3** and **5** contain the same sequence of chromophores, their CD spectra should be directly comparable. The relative CD intensities of **5** and **3** at their maxima around 385 nm indicate an 80/20 ratio[‡] of *M*- to *P*-diastereomers for **5** (Fig. S3, ESI[†]), which matches the ratio observed by ¹H NMR. Taking this ratio into consideration, an energy difference between the handedness bias induced by **B**^{Rme} and Camph of about −3.4 kJ mol^{−1} can be derived.

When two **B**^{Rme} units cooperate to bias handedness in the same sequence, as in **6**, we find that the effect of a terminal (*S*)-Camph is completely reversed. A main species is observed by ¹H NMR, and CD confirms *M* handedness (Fig. 3). The CD intensity of **6** also matches that of **7**, which lacks the camphanlyl group. Minor signals in the ¹H NMR spectra of **6** and **7** were observed that can be assigned to the incomplete enantiomeric purity of **B**^{Rme} arising from the enantiomeric purity of the lactate precursor. A small amount of one or the other chiral **B** unit may have (*S*) stereochemistry opposite to the (*R*) configuration of **B**^{Rme}. In these cases, the effect of **B**^{Rme} and that of **B**^{Sme} would cancel each other and the camphanlyl group would favor *P* helicity, leading to small amounts of (*S,R,S*)-*P* and (*S,S,R*)-*P* diastereomeric conformers of **6** and (*S,R*)-*P/M* and (*R,S*)-*P/M* conformers of **7**, where the bias of Camph is missing.

In conclusion, quantitative handedness bias was achieved in water, methanol, and DMSO by placing the new **B**^{Rme} monomer within a quinoline helix. The energy difference was greater than that generated by the Camph group. The bias could be further enhanced by incorporating more than one **B**^{Rme} unit within the same helix. The handedness bias was not complete only when **B**^{Rme} was placed near the C-terminus. Full handedness control could thus be achieved without any modifications at either the N- or C-terminus, allowing for further functionalization at both ends of the helix. Being able to avoid bulky handedness-inducing groups at the N- or C-terminus will also be beneficial to water solubility, as Camph, Pin, and Oxaz are all lipophilic. These combined features will be useful for protein surface recognition using helical foldamers. B units also provide a new means to introduce side chains at the stereogenic center. This prospect and the effect of multiple B units on the helix geometry are being investigated and will be reported in due course.

Synchrotron data were collected at beamline P14 operated by EMBL Hamburg at the PETRA III storage ring (DESY, Hamburg, Germany). We thank Dr Saravanan Panneerselvam for his assistance in using the beamline.

Conflicts of interest

There are no conflicts to declare.

Notes and references

[‡] The total CD intensity results from the sum of the CD signals of *P*- and *M*-isomers, which have opposite signs. Therefore, the 40% lower CD

intensity observed for **5** in comparison to **3** reflects an 80/20 ratio of *M*- to *P*-isomers

- 1 E. Merlet, K. Moreno, A. Tron, N. McClenaghan, B. Kauffmann, Y. Ferrand and C. Olivier, *Chem. Commun.*, 2019, **55**, 9825–9828.
- 2 D. Zheng, L. Zheng, C. Yu, Y. Zhan, Y. Wang and H. Jiang, *Org. Lett.*, 2019, **21**, 2555–2559.
- 3 L. Zheng, D. Zheng, Y. Wang, C. Yu, K. Zhang and H. Jiang, *Org. Biomol. Chem.*, 2019, **17**, 9573–9577.
- 4 G. Lautrette, B. Wicher, B. Kauffmann, Y. Ferrand and I. Huc, *J. Am. Chem. Soc.*, 2016, **138**, 10314–10322.
- 5 S. Saha, B. Kauffmann, Y. Ferrand and I. Huc, *Angew. Chem., Int. Ed.*, 2018, **57**, 13542–13546.
- 6 J. M. Alex, V. Corvaglia, X. Hu, S. Engilberge, I. Huc and P. B. Crowley, *Chem. Commun.*, 2019, **55**, 11087–11090.
- 7 P. S. Reddy, B. Langlois d'Estaintot, T. Granier, C. D. Mackereth, L. Fischer and I. Huc, *Chem. – Eur. J.*, 2019, **25**, 11042–11047.
- 8 M. Vallade, M. Jewginski, L. Fischer, J. Buratto, K. Bathany, J.-M. Schmitter, M. Stupfel, F. Godde, C. D. Mackereth and I. Huc, *Bioconjugate Chem.*, 2019, **30**, 54–62.
- 9 M. Vallade, P. Sai Reddy, L. Fischer and I. Huc, *Eur. J. Org. Chem.*, 2018, **57**, 5489–5498.
- 10 J. Buratto, C. Colombo, M. Stupfel, S. J. Dawson, C. Dolain, B. Langlois d'Estaintot, L. Fischer, T. Granier, M. Laguerre, B. Gallois and I. Huc, *Angew. Chem., Int. Ed.*, 2014, **53**, 883–887.
- 11 E. Yashima, N. Ousaka, D. Taura, K. Shimomura, T. Ikai and K. Maeda, *Chem. Rev.*, 2016, **116**, 13752–13990; Z. Liu, X. Hu, A. M. Abramyan, Á. Mészáros, M. Csekei, A. Kotschy, I. Huc and V. Pophristic, *Chem. – Eur. J.*, 2017, **23**, 3605–3615; A. Zhang, Y. Han, K. Yamato, X. C. Zeng and B. Gong, *Org. Lett.*, 2006, **8**, 803–806.
- 12 A. M. Kendhale, L. Poniman, Z. Dong, K. Laxmi-Reddy, B. Kauffmann, Y. Ferrand and I. Huc, *J. Org. Chem.*, 2011, **76**, 195–200.
- 13 Li Yang, M. Chunmiao, B. Kauffmann, L. Dongyao and Q. Gan, *Org. Biomol. Chem.*, 2020, **18**, 6643–6650.
- 14 L. Zheng, Y. Zhan, C. Yu, F. Huang, Y. Wang and H. Jiang, *Org. Lett.*, 2017, **19**, 1482–1485.
- 15 Y. Inai, Y. Kurokawa and N. Kojima, *J. Chem. Soc., Perkin Trans. 2*, 2002, 1850–1857; Y. Inai, Y. Kurokawa and T. Hirabayashi, *Biopolymers*, 1999, **49**, 551–564; M. D. Poli, M. D. Zotti, J. Raftery, J. A. Aguilar, G. A. Morris and J. Clayden, *J. Org. Chem.*, 2013, **78**, 2248–2255; R. A. Brown, T. Marcelli, M. D. Poli, J. Sola and J. Clayden, *Angew. Chem., Int. Ed.*, 2012, **51**, 1395–1399.
- 16 Z. Dong, G. P. A. Yap and J. M. Fox, *J. Am. Chem. Soc.*, 2007, **129**, 11850–11853.
- 17 H.-Y. Hu, J.-F. Xiang, Y. Yang and C.-F. Chen, *Org. Lett.*, 2008, **10**, 69–72.
- 18 E. Kolomiets, V. Berl and J.-M. Lehn, *Chem. – Eur. J.*, 2007, **13**, 5466–5479.
- 19 M. Kudo, V. Maurizot, B. Kauffmann, A. Tanatani and I. Huc, *J. Am. Chem. Soc.*, 2013, **135**, 9628–9631.
- 20 M. Akazome, Y. Ishii, T. Nireki and K. Ogura, *Tetrahedron Lett.*, 2008, **49**, 4430–4433.
- 21 N. Delsuc, F. Godde, B. Kauffmann, J.-M. Léger and I. Huc, *J. Am. Chem. Soc.*, 2007, **129**, 11348–11349.
- 22 C. Dolain, J. M. Leger, N. Delsuc, H. Gornitzka and I. Huc, *Proc. Natl. Acad. Sci. U. S. A.*, 2005, **102**, 16146–16151.
- 23 D. Sánchez-García, B. Kauffmann, T. Kawanami, H. Ihara, M. Takafuji, M.-H. I. n. Delville and I. Huc, *J. Am. Chem. Soc.*, 2009, **131**, 8642–8648.
- 24 B. Baptiste, C. Douat-Casassus, K. Laxmi-Reddy, F. Godde and I. Huc, *J. Org. Chem.*, 2010, **75**, 7175–7185.
- 25 X. Hu, S. J. Dawson, Y. Nagaoka, A. Tanatani and I. Huc, *J. Org. Chem.*, 2016, **81**, 1137–1150.
- 26 C. Dolain, H. Jiang, J.-M. Léger, P. Guionneau and I. Huc, *J. Am. Chem. Soc.*, 2005, **127**, 12943–12951.
- 27 C. C. McDonald and W. D. Phillips, *J. Am. Chem. Soc.*, 1967, **89**, 6332–6341.
- 28 G. W. Collie, K. Pulka-Ziach, C. M. Lombardo, J. Fremaux, F. Rosu, M. Decossas, L. Mauran, O. Lambert, V. Gabelica, C. D. Mackereth and G. Guichard, *Nat. Chem.*, 2015, **7**, 871–878.